

Shell-Solid FEM Model of a Violin Resonance Body

Andrzej KABALA

Poznan University of Technology, Faculty of Mechanical Engineering,
3 Piotrowo, 60-965 Poznań, kabalaandrzej@gmail.com

Roman BARCZEWSKI

Poznan University of Technology, Faculty of Mechanical Engineering
3 Piotrowo, 60-965 Poznan, roman.barczewski@put.poznan.pl

Abstract

The FEM model of a violin resonance body presented in the article has been developed in order to simulate various issues in the field of violin dynamics and vibro-acoustics. All violin parts participating in the vibrations of the resonance body (solid and shell parts) are included in the model. Material properties and material orientation (anisotropy) of wood species used to make the violin parts have been taken into account in the model. Properties of spruce have been applied to the top plate (with *f*-holes) and solid parts. Properties of maple have been applied to the back plate, ribs and bridge. Two basic problems were considered: simulation and analysis of violin body vibrations in the cases of natural vibrations (**Frequency*) and forced vibrations - excited by strings (**Steady-state dynamics*). The results of simulations have been described and illustrated.

Keywords: violin body modelling, violin bridge, vibration modes, harmonic excitations

1. Introduction

The main task of a violin resonance body is to generate sound, the quality of which largely results from the vibroacoustic properties of the body. Therefore, while developing the model of the violin body, efforts have been made to reproduce the geometry of the violin as faithfully as possible and to take into account the properties of the materials from which the violin body parts are made. It is worth mentioning that interaction between surfaces of wooden parts of the violin body and air that surrounds them determine amplitudes of velocities and phase angles of vibrations on the contact surfaces of solid parts and air. The article contains some selected simulation results in which the mutual interaction between wood elements and air was omitted. The model of the violin body (in the presented variant) does not include a soundpost. Its effect on the vibration of violin body has been omitted. Only the resonance body of the violin was the subject of dynamic tests (simulations). The elaborated FE model of the violin resonance body was used in two aspects:

- determination of the first 15 natural frequencies and vibration modes (using the ABAQUS® ** Frequency* option),
- simulation of the response of the violin body to harmonic excitations by vibrating string and determination of vibration modes (using the ABAQUS® - ** Steady-state dynamics* option).

Simulation results have been presented graphically. On their basis, it was possible to carry out the appropriate comparison, observations as well as to formulate conclusions.

2. Violin resonance body

In his publications C. Gough reports the use of shell elements for modeling the body of a violin [1-3]. A similar type of modeling was used in the research conducted by Jansson, Barczewski, and Kabała [4]. The presented model of the resonance body of a violin (Fig. 1a) consists both of solid parts (Fig. 1b) and shell parts (Fig. 1c). Although the shell parts of the violin in an energetic sense contribute mostly to the sound generation, the solid parts must not be omitted because they also contribute to the vibration of the violin body. For this reason, all parts both solid and shell type should be included in the FE model. The basic dimensions of the violin resonance body, which were taken into account in the development of the FE model, are shown in Fig. 2. Typically two different materials (different wood species) are used to make the violin resonance body parts. In the developed FE model it was assumed that the top plate (with f-holes) and all solid parts are made of spruce and the other parts (back plate, bridge, ribs) are made of maple. The model also takes into account the material orientation of all parts of the violin body. The bridge has a very important function in the violin [4-7]. Vibrations of the violin strings at the top of the bridge are transmitted through the feet of the bridge to the top plate of the violin (the bridge island).

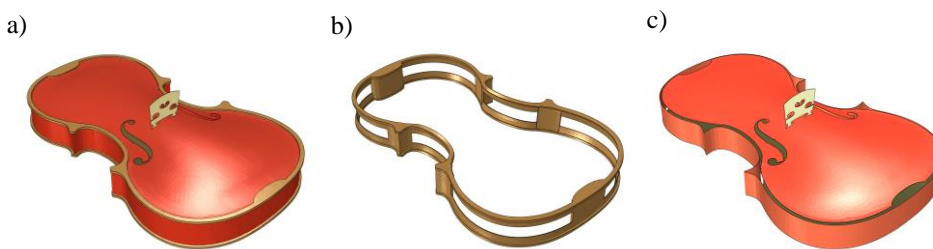


Figure 1. The violin resonance body (a), solid parts of the body (b), the shell parts (c)

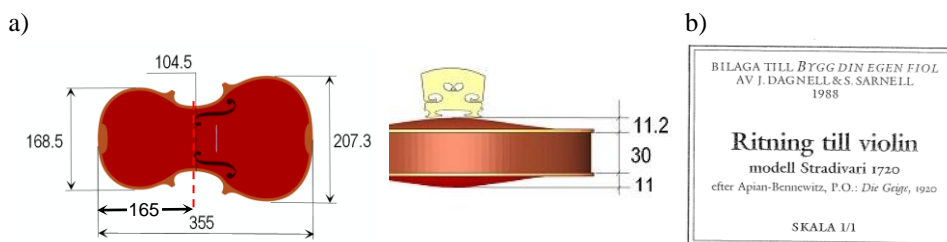


Figure 2. Basic dimensions of the violin resonance body [mm] (a), a source of information about the geometry of the violin (b)

3. FEM model

The basis for the development of the FEM model of the violin resonance body were dimensions and geometry obtained from documentation (see Fig. 2b) as well as work of S. Muratov [8]. The solid parts and the shell parts of the violin resonance body are shown in Figure 1. The geometry of the model was obtained by connecting (*constraints*) the adjacent parts. Two wooden materials, spruce and maple were applied. The properties of materials were sourced from E. K. Askenazi [9].

Table 1. Material properties of wood that were taken into account in the development of the FEM model of the violin resonance body [9]

	Density kg/m ³	Young's modulus [GPa]			Shear modulus [GPa]			Poisson's ratios		
		E_1	E_2	E_3	G_{12}	G_{13}	G_{23}	ν_{12}	ν_{13}	ν_{23}
spruce	590	16.225	0.701	0.4	0.645	0.416	0.347	0.44	0.33	0.42
maple	500	10.2	1.55	0.89	1.158	1.132	0.287	0.46	0.5	0.82

Properties of spruce have been applied to the top plate (with f-holes) and solid parts. Properties of maple have been applied to the back plate, ribs and bridge. Material orientations were defined for all parts individually (see examples - Fig. 4). Uniform thicknesses of the following parts were assumed: the top plate (with f-holes) is 3 mm thick, the back plate is 3 mm thick and the ribs are 1.25 mm thick. The bridge has no uniform thickness. The thickness of the bridge is determined by the nodal thickness and decreases linearly along with the height of the bridge from 4 mm (feet) to 1.4 mm (the bridge top).

Research issues

Step 1: 15 modes of the natural frequencies (**Frequency*),

Step 2: (**Steady-state dynamics*) – vibrations of the violin body – harmonically forced (excitation by vibrations of the violin strings G, D, A, E and the corresponding frequencies).

Interaction – *Tie constraint* and *Shell-to-solid coupling constraint* were used to connect the violin parts.

Boundary conditions – Figure 5 b, c show load, and boundary conditions. The harmonic excitation of the bridge by the vibrated string is transferred to the upper plate (with *f-holes*) through the feet of the bridge (see Fig. 5b). The following amplitudes of the forces were assumed: $F_y = 0.1$ N and $F_z = 0.02$ N. The frequencies of violin strings that were considered in the simulations are presented in Table 2.

Table 2. The frequencies of violin strings that were considered in the simulations

Excitation frequencies range [Hz]		
<i>lower</i>	<i>nominal</i>	<i>upper</i>
195.0	“Sol” 196.0 string G	197.0
292.7	“Re” 293.7 string D	294.7
439.0	“La” 440.0 string A	441.0
658.3	“Mi” 659.3 string E	660.3

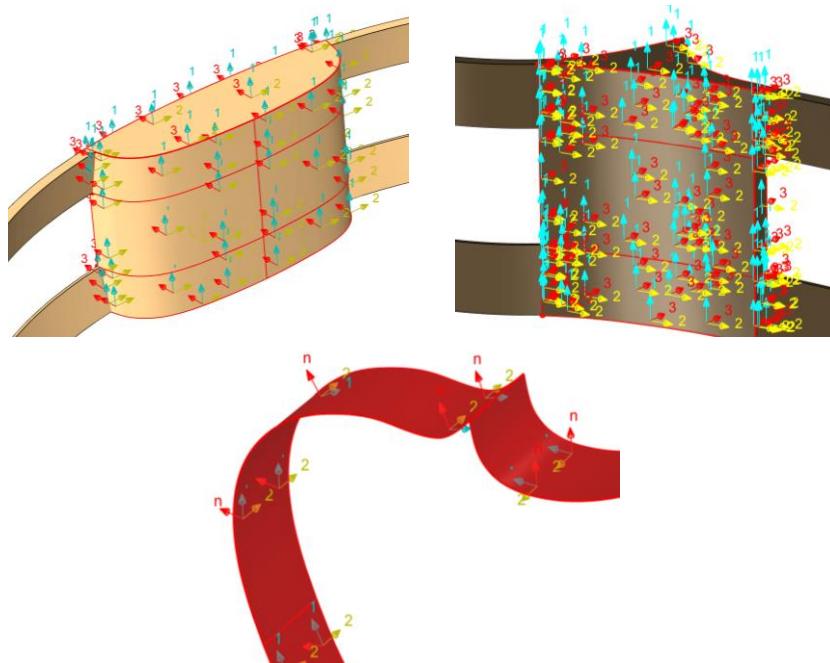


Figure 4. Examples of material orientation marking

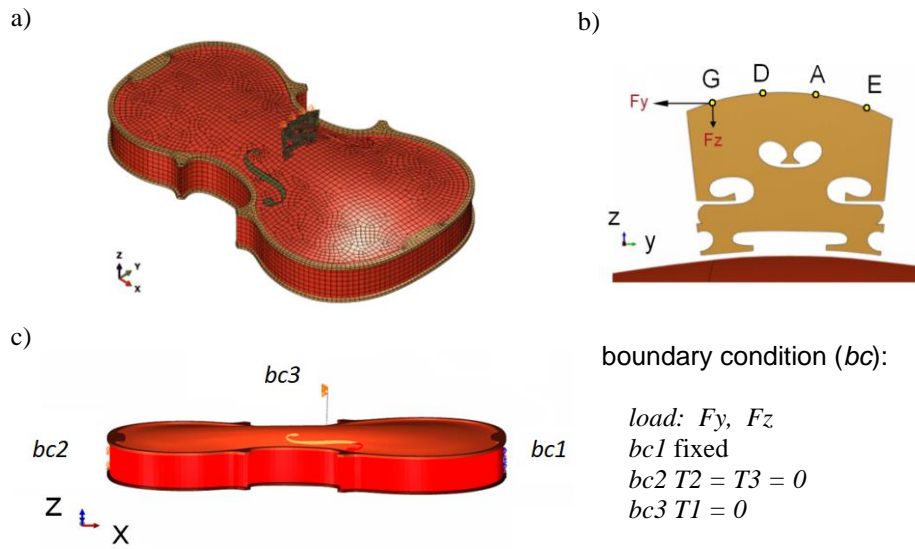


Figure 5. The violin resonance body FE model: mesh (a), boundary condition (b, c)

Three boundary conditions were adopted (see Fig. 5c):

- *bc1* (region Chinrest and Button) – all translation and rotation are locked,
- *bc2* (Neck side) – translation $T_2 = T_y = 0$, $T_3 = T_z = 0$,
- *bc3* (points of contact of the strings with the bridge) $T_1 = T_x = 0$.

FE mesh (see Fig. 5a). The shell parts of the violin were modeled with S4R type elements (dominant type of element) and S3 type elements (applied locally), while the solid parts of the violin body were modeled with C3D8R elements.

Summarizing the above assumptions and parameters regarding the FEM model:

- shell parts and solid parts were used to build the model,
- two wooden materials – spruce and maple were applied,
- the properties of both materials were defined by the Young's modulus E_1 , E_2 , E_3 , the shear modulus G_{12} , G_{13} , G_{23} and the Poisson's ratios ν_{12} , ν_{13} , ν_{23} ,
- the material orientations were defined for all parts – see examples in Fig. 4,
- the *tie constraints* and the *shell-to-solid coupling constraints* were applied to connect selected surfaces of the parts.

4. Results of the simulations

The simulations carried out in the first step (*Step 1 *Frequency*) concerned the first 15 vibration modes. The modes' frequencies are shown in Table 3, additionally, four shapes of selected modes are shown in Figure 6.

Table 3 The frequencies of the first 15 vibration modes of the violin body

Mode No.	#1	#2	#3	#4	#5	#6	#7	#8
Frequency [Hz]	108.4	239.4	276.2	346.2	439.2	450.9	505.8	571.2
Mode No.	#9	#10	#11	#12	#13	#14	#15	
Frequency [Hz]	577.3	595.7	676.0	718.7	849.0	883.4	907.3	

In the second step (*Step 2 - *Steady-state dynamics*) the harmonic excitation was used to simulate the response of the violin body in the FE model. The excitation frequencies corresponded to the natural frequencies of the G, D, A, E strings. Nevertheless, the simulations were also performed in the frequency ranges shown in Table 2. Figure 7 shows four response shapes of the developed violin FE model to monoharmonic excitation by single strings (string frequencies: G - 196.0 Hz, D - 293.7 Hz, A - 440 Hz, E - 659.3 Hz). Figure 8 shows the shape of the resonance body vibrations in a cross-section at a distance of 165 mm from the violin neck attachment place (see Fig. 2a).

The *bridge island* has different displacement shapes. In the case of natural vibrations, the shapes change according to the modes (see Fig. 6). In the case of harmonic excitations, the bridge and the bridge island also oscillate harmonically, but other regions have their own shapes depending on the excitation frequency (see Fig. 7).

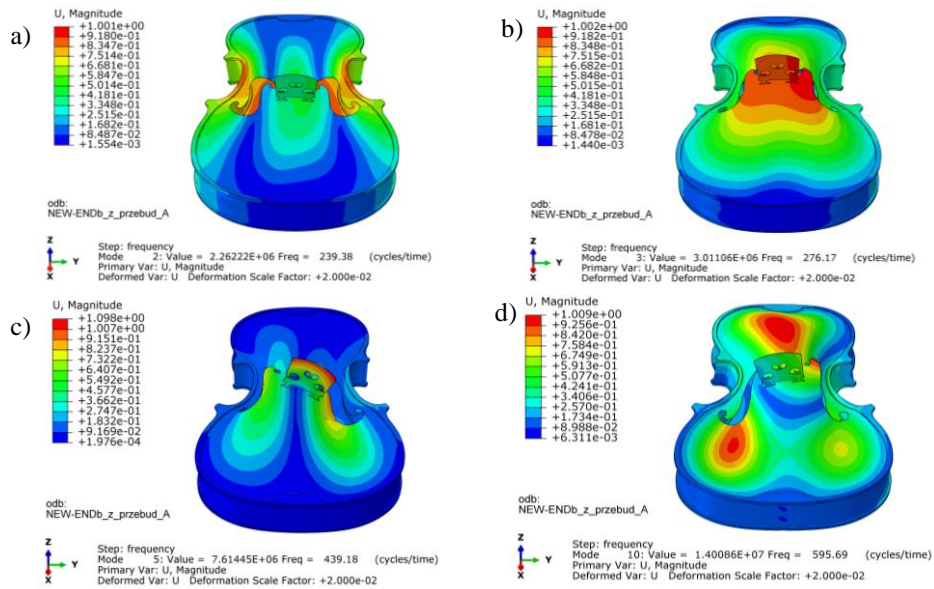


Figure 6. Selected vibration modes - natural frequencies (**Frequency*)
 a) mode #2 - 239 Hz, b) mode #4 - 276 Hz, c) mode #5 - 439 Hz, d) mode #10 - 596 Hz

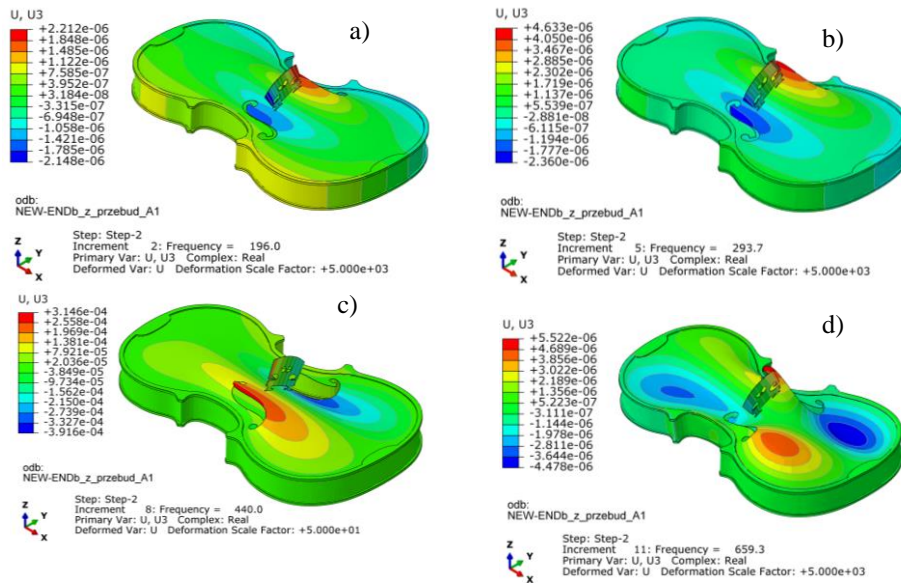


Figure 7. Harmonic excitation (**Steady-state dynamics, Direct*); Primary Var.: U, U3.
 a) 196 Hz - string G, b) 293.7 Hz - string D, c) 440 Hz - string A, d) 659.3 Hz - string E

A large increase in displacement can be observed when the excitation frequency is equal or near to the frequency of the mode. For example, it can be seen that mode 5 (see Fig. 6c) has 439.18 Hz and the forced vibration by the A string has a very close frequency equal to 440 Hz (see Fig 7c, Fig. 8c and Fig. 9). The Deformation Scale Factor increases about 100 times (the amplitude of displacements increases) for a frequency of 440 Hz. The phase angle also changes (see Fig. 8 and Fig. 9). Figure 9 shows the changes in the displacement amplitude and phase angle of the bridge corner (E string side) in the frequency range from 150 to 1000 Hz.

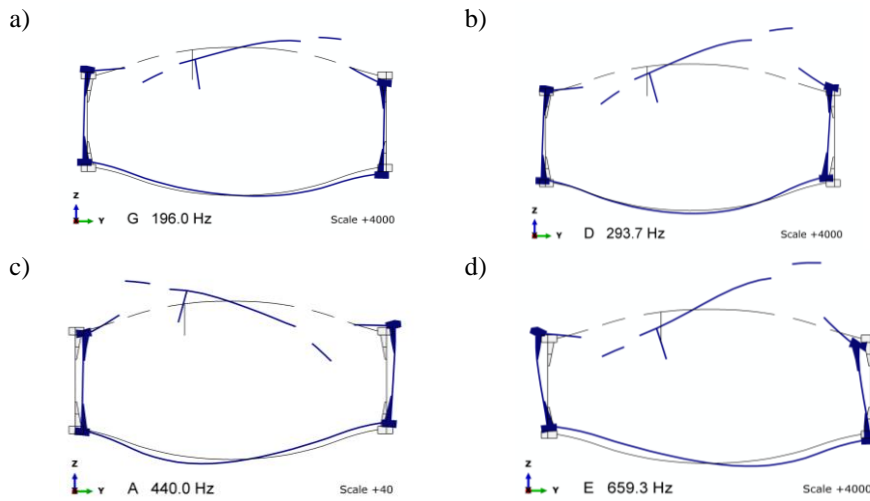


Figure 8. Shape of the violin body vibrations in a cross-section at a distance of 165 mm from the neck attachment place; Harmonic excitation (*Steady-state dynamics); a) 196 Hz (string G) - scale 4000, b) 293.7 Hz (string D) - scale 4000, c) **440 Hz** (string A) - **scale 40**, d) 659.3 Hz (string E) - scale 4000

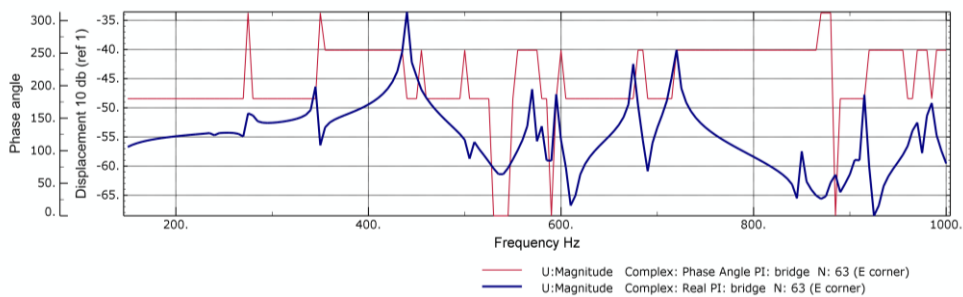


Figure 9. Harmonic excitation (*Steady-state dynamics, Direct); Response (U Magnitude) - the bridge corner (E string side), frequency range: 150 – 1000 Hz

5. Conclusions

The presented simulations were used to test the correctness of the FEM model (especially in the aspect shell-solid connections). The simulation results confirmed the correctness of the modeling.

The introduction of solid parts in the model brought the FEM model much closer to the modeled resonance body of a violin by taking into account the spatial distribution of masses and the material properties of the solid part.

The introduction of harmonic excitations (**Steady-state dynamics, Direct*) by the vibrating strings showed the dominant role of the bridge in transferring vibrations to the violin resonance body. The form of vibrations (bridge and bridge island) is similar for all excitation frequencies. The differences in the forms of vibrations, depending on the excitation frequency, occur in regions beyond the "bridge island".

Omitting the damping in the graph (Fig. 9) results in a large range of amplitude changes in the frequency range 400-1000 Hz. The diagram shows the displacement modules of the bridge corner (E string side). Noteworthy is the resonance peak at 440 Hz, resulting from the convergence of the natural frequency (439.18 Hz) and the excitation frequency (by string A - 440 Hz).

It is necessary to conduct more extensive research, that would take into account the coupling between the surfaces of the resonance body and the air volume inside violin body, since the interaction between them is crucial in generation of sound by a violin.

Acknowledgment

This paper was partially financially supported by research project 0612/SBAD/3567.

References

1. C. Gough, *The violin bridge-island input filter*, Journal of the Acoustical Society of America 143 (2018) 113 – 123.
2. C. Gough, *Violin Acoustics, The acoustics of thin-walled shallow boxes – a tale of coupled oscillators*, Acoustics Today, 12(2) (2016) 22 – 30.
3. C. Gough, *A violin shell model: Vibrational modes and acoustics*, Journal of the Acoustical Society of America 137(3) (2015) 1210 – 1225.
4. E. V. Jansson, R. Barczewski, A. Kabala, *On the violin bridge hill – comparison of experimental testing and FEM*. *Vibration in Physical Systems*, 27 (2016) 151 – 160.
5. F. Durup, E. V. Jansson, *The quest of the violin bridge hill*. *Acta Acustica united with Acustica* 91 (2005) 206 – 213.
6. J. Woodhouse, *On the "Bridge hill" of the Violin*, *Acta Acustica united with Acustica*, 91 (2005) 155 – 165.
7. J. Woodhouse, *The acoustics of the violin: a review*, *Reports on Progress in Physics*. 77 (2014) 1 – 96 (44).
8. S. Muratov, *The Art of the Violin Design*, AuthorHouse, 2002.
9. E. K. Askenazi, *Anisotropy of woods and wood materials*, Forest industry ("Lesnaiia Promyslennost"), Moscow 1978.